

# CODING OF TIME-VARYING HORMONAL SIGNALS IN INTRACELLULAR CALCIUM SPIKE TRAINS

K. PRANK, C. SCHÖFL, L. LÄER, M. WAGNER, A. VON ZUR MÜHLEN,  
G. BRABANT

*Department of Clinical Endocrinology, Medical School Hannover,  
Carl-Neuberg-Str. 1, D-30625 Hannover, Germany*

F. GABBIANI

*Computation and Neural Systems Program, 139-74 Division of Biology,  
California Institute of Technology, Pasadena, California 91125, USA*

In a variety of cell types extracellular hormonal stimuli varying in time are transferred across the cell membrane into repetitive spikes of the intracellular calcium concentration ( $[Ca^{2+}]_i$ ). Distinct temporal patterns of  $[Ca^{2+}]_i$  spikes are capable of regulating the function and structure of target cells. Here, we investigate the ability of transmembrane signaling to encode time-varying hormonal stimulations (bandlimited Gaussian white noise) in a model of receptor-controlled  $[Ca^{2+}]_i$  oscillations. The encoding of hormonal signals in  $[Ca^{2+}]_i$  spike trains is quantified by using an information-theoretic approach allowing to estimate the hormonal stimulus from  $[Ca^{2+}]_i$  spike trains. Our results suggest that intracellular  $[Ca^{2+}]_i$  spike trains convey faithful information on temporal variations of extracellular hormonal concentrations at scales of 30–200 sec, corresponding to cut-off frequencies between 5 and 30 mHz of the random hormonal stimulation.

## 1 Introduction

### 1.1 Information Transmission and Processing in Endocrine Systems

In biology information is transmitted over long distances by the nervous system and the endocrine system. For endocrine signaling, a hormone secreted by a cell is transported via the blood stream to distant target cells where it produces a distinct response after binding to a specific receptor. The cellular response upon binding of a hormonal ligand to its receptor is mediated by a variety of intracellular second messenger pathways<sup>1</sup>. The  $Ca^{2+}$ –phosphatidylinositol (PI) signaling pathway plays a major role in transmembrane signal transmission<sup>2</sup> for a large number of different cell types. In this pathway hormonal stimuli lead to the formation of inositol (1,4,5)–trisphosphate ( $IP_3$ ) which triggers the release of  $Ca^{2+}$  from internal stores. Succeeding negative feedback mechanisms lead to a fall of  $[Ca^{2+}]_i$  back to resting levels. The result are repetitive  $[Ca^{2+}]_i$  transients varying in frequency and amplitude depending on the strength and type of the hormonal stimulus.  $[Ca^{2+}]_i$  spike trains have been demonstrated to allow for the differential regulation of distinct cellular re-

sponses<sup>3</sup>, such as the activation of protein kinases<sup>4</sup> as well as the regulation of transcription<sup>5</sup>, differentiation<sup>6</sup>, motility, and morphology<sup>7</sup>. The generation of  $[Ca^{2+}]_i$  oscillations has been studied experimentally and theoretically mostly under constant hormonal stimulation. However, it has been demonstrated that almost all hormones are secreted in a burstlike or pulsatile manner resulting in a time-varying concentration in the blood stream<sup>8,9</sup>.

Motivated by these results, Schöfl *et al.*<sup>10</sup> performed experiments in liver cells which demonstrated the mapping of periodic time-varying hormonal stimuli with phenylephrine (an  $\alpha_1$ -adrenoreceptor agonist) into distinct temporal patterns of  $[Ca^{2+}]_i$  spike trains. Furthermore, a modulation of the  $[Ca^{2+}]_i$  spike amplitude by the frequency of the periodic hormonal stimulus could be observed. Motivated by this study, Chay *et al.*<sup>11</sup> adapted a mathematical model for receptor-controlled  $[Ca^{2+}]_i$  oscillations which had been numerically studied only under constant agonist stimulation<sup>12</sup>. This new model accounts for most of the dynamical features observed in the experiments of Schöfl *et al.*<sup>10</sup> such as blocked and delayed  $[Ca^{2+}]_i$  responses to the extracellular stimulus. Transmembrane signaling in this model system has only been studied experimentally<sup>10</sup> and numerically<sup>11</sup> using periodic stimuli, whereas in the physiological situation secretory pulses and the resulting fluctuations of hormone concentration in the blood stream and tissue are usually not equally spaced<sup>8,13</sup>. Thus, we investigated numerically transmembrane signaling using bandlimited Gaussian white noise stimuli in the model for receptor-controlled  $[Ca^{2+}]_i$  oscillations proposed by Chay *et al.*<sup>11</sup>. The objective of this study was to quantitatively characterize the impact of transmembrane transduction on the flow of time-varying information from the external hormonal signals to the final effector systems of the cell.

## 1.2 Information Encoding in Sensory Neuronal Systems

This study was motivated by experimental and numerical studies on the information flow in sensory neuronal systems<sup>14–19</sup> where the question of *temporal coding* of information in spike trains has recently received renewed attention. Most of the information in the arrival times of action potentials in the nervous system is neglected when studying the mean firing rate (*mean rate coding*) as the relevant parameter characterizing the neuronal response. The basic idea of *temporal coding* is that spike timing plays an important role in encoding various aspects of the stimulus. This has been demonstrated in a number of different sensory systems<sup>14,15,20–26</sup>. Thus *temporal coding* may be used to increase the efficacy of information transfer.

## 2 Methods

### 2.1 Receptor-Controlled Model for $[Ca^{2+}]_i$ Oscillations

This study is based on the model proposed by Chay *et al.*<sup>11</sup> which assumes that the receptor-controlled  $[Ca^{2+}]_i$  spikes are caused by the increase of activated guanosine-5'-triphosphate-(GTP) binding proteins (g-GTP) which in combination with positive feedback processes and cooperative effects activates phospholipase C (PLC). Activated PLC converts phosphatidylinositol(4,5)-bisphosphate ( $PtdIP_2$ ) into diacylglycerol (DAG) and inositol (1,4,5)-trisphosphate ( $IP_3$ ) which triggers the release of  $Ca^{2+}$  from the endoplasmic reticulum (ER) by binding to the specialized tetrameric  $IP_3$  receptor in the ER membrane. The level of cytosolic  $Ca^{2+}$  drops fast as  $Ca^{2+}$  is pumped back into the ER. Numerical simulations of this model performed so far have used only periodically delivered square pulses without assuming any randomness in the stimulatory pattern. These pattern are far from the physiologically and pathophysiologicaly observed dynamics of pulsatile hormone secretion<sup>8,13</sup>. Thus we used bandlimited Gaussian white noise stimuli as a first approximation to the temporal variations occuring in natural patterns. The model of Chay *et al.* comprises the simulation of phospholipase C (PLC), diacylglycerol (DAG), and  $G_\alpha - GTP$  time series to generate  $[Ca^{2+}]_i$  spike trains and is summarized by the following equations:

$$\frac{d[G_\alpha - GTP]}{dt} = k_g[G_\alpha - GDP] - 4k_p[G_\alpha - GTP]^4[PLC] - h_g[G_\alpha - GTP], \quad (1)$$

$$\frac{d[DAG]}{dt} = k_d[PLC^*] - h_d[DAG] + l_d, \quad (2)$$

$$\frac{d[Ca^{2+}]_i}{dt} = \rho \left\{ k_c \frac{[IP_3]^3}{K_s^3 + [IP_3]^3} - h_c[Ca^{2+}]_i + l_c \right\}, \quad (3)$$

$$\frac{d[PLC^*]}{dt} = k_p[G_\alpha - GTP]^4[PLC] - h_p[PLC^*]. \quad (4)$$

Eq. 1 describes the change of  $[G_\alpha - GTP]$  due to the conversion of  $G_\alpha - GDP$  to  $G_\alpha - GTP$ . In eq. 1,  $k_g$  is equated to the time-varying agonist concentration<sup>11</sup> (in units of  $sec^{-1}$ ). The three kinetic parameters  $k_p, h_p, k_d$  are assumed to take the following forms:

$$k_n = k'_n \frac{[DAG]^2}{K_D^2 + [DAG]^2}, \quad (5)$$

where  $k_n = k_p, h_p$  or  $k_d$  and  $k'_p = 2 \times 10^{-7} \text{ nM}^{-4} \text{ sec}^{-1}$ ,  $h'_p = 0.5 \text{ sec}^{-1}$ ,  $k'_d = 700 \text{ sec}^{-1}$ . The remaining kinetic constants are  $K_D = 25 \text{ nM}$  and  $h_g$  which

is set to  $0.0 \text{ sec}^{-1}$  in a first approximation. Eq. 2 models the change of DAG and  $IP_3$  ( $h_d = 100 \text{ sec}^{-1}$ ,  $l_d = 250 \text{ nM sec}^{-1}$ ). For simplicity it is assumed that  $[DAG]$  and  $[IP_3]$  increase with the same rate. Eq. 3 describes the change of intracellular calcium concentration  $[Ca^{2+}]_i$  ( $\rho k_c = 9.0 \times 10^4 \text{ nM sec}^{-1}$ ,  $K_s = 300 \text{ nM}$ ,  $\rho h_c = 1.0 \text{ sec}^{-1}$ ,  $\rho l_c = 200 \text{ nM sec}^{-1}$ ). The first term in the curly brackets models the release of  $Ca^{2+}$  from the endoplasmic reticulum (ER). Eq. 4 models the formation of activated PLC ( $PLC^*$ ) from PLC through the action of  $G_\alpha - GTP$ . The second term describes the loss of ( $PLC^*$ ) by the hydrolysis of the complex to  $G_\alpha - GDP$ .

A qualitative explanation for the generation of  $[Ca^{2+}]_i$  spike trains in this model is as follows:  $Ca^{2+}$  is released from intracellular  $Ca^{2+}$  stores (such as the ER) when  $[G_\alpha - GTP]$  and thus  $[IP_3]$  reaches a critical threshold level. The  $Ca^{2+}$  response is blocked when  $[G_\alpha - GTP]$  is too low and the agonist stimulus is delivered prematurely. Each  $[Ca^{2+}]_i$  spike train,  $x(t)$ , was simulated for 240,000 sec on a Sun SPARCstation 20 using source code written in MATLAB (MathWorks Inc., Natick, MA). The system of differential equations was integrated using a modified Rosenbrock formula stiff solver (variable integration time step). The stimulus,  $s(t) + s_{mean}$ , which corresponds to  $k_g$  in the Chay *et al.* model, was generated by low-pass filtering uncorrelated zero-mean, unit variance Gaussian white noise, and then rescaling this signal to the interval  $[0 \text{ sec}^{-1}; 0.03 \text{ sec}^{-1}]$ . The average value of  $k_g$  is  $s_{mean} = 0.015 \text{ sec}^{-1}$ . Filtering was performed in the frequency domain, by setting Fourier coefficients above the desired cut-off frequency,  $f_c$ , of the stimulus,  $s(t)$ , to zero. The cut-off frequency  $f_c$  ranged from 3 mHz to 100 mHz.

In a second step we choose a fixed cut-off frequency of 10 mHz and varied the maximum stimulus amplitude between 0.015 to  $0.060 \text{ sec}^{-1}$  to investigate the impact of increasing mean  $Ca^{2+}$  spike frequency on the coding performance.

## 2.2 Stimulus Estimation from $[Ca^{2+}]_i$ Spike Trains

The ability of neuronal spike trains to convey precise information about the temporal dynamics of a random bandlimited stimulus, such as the hormonal stimulation  $s(t)$  considered above, has been studied using information-theoretic approaches. Methods from stochastic estimation theory<sup>27,28</sup> allow to compute a temporal filter  $h(t)$  that, when convolved with a spike train in response to the stimulus,  $s(t)$ , will produce an estimate  $s_{est}(t)$  of  $s(t)$ . Thus, part of the temporal dynamics of the stimulus can be reconstructed from the spike train. These stimulus reconstruction methods have been introduced into the field of

neuroscience by Bialek and collaborators to explore the information transmission by peripheral sensory neurons in a variety of preparations<sup>14,29</sup>.

To estimate the information about time-varying hormonal concentration encoded in  $[Ca^{2+}]_i$  spike trains in our simulations, we used the following stimulus reconstruction algorithm<sup>14,16,30</sup>.

Let

$$x(t) = \sum_i \delta(t - t_i) - x_0 \quad (6)$$

be the  $[Ca^{2+}]_i$  spike train with the mean value,  $x_0$ , subtracted. In eq. 6 the  $t_i$ 's denote the occurrence times of  $Ca^{2+}$  spikes in response to the Gaussian stimulus,  $s(t)$ . A linear estimate,  $s_{est}(t)$ , of the stimulus,  $s(t)$ , given the spike train, is calculated by convolving the  $[Ca^{2+}]_i$  spike train with a filter,  $h(t)$ :

$$s_{est}(t) = \int_0^T dt' h(t - t') x(t'). \quad (7)$$

The filter,  $h(t)$ , is to be chosen in such a way as to minimize the mean square error,  $\epsilon^2$ , between the stimulus and estimate

$$\epsilon^2 = \frac{1}{T} \int_0^T dt [s(t) - s_{est}(t)]^2, \quad (8)$$

where the integration is over the duration of the simulation ( $T = 240,000$  sec). Solving for the filter  $h(t)$  leads to

$$h(t) = \int_{-f_c}^{f_c} df \frac{S_{sx}(-f)}{S_{xx}(f)} e^{-i2\pi ft}. \quad (9)$$

In this equation,  $f_c$  is the cut-off frequency of the stimulus,  $S_{sx}(f)$  represents the Fourier transform of the cross-correlation between the stimulus and the spike train and  $S_{xx}(f)$  the Fourier transform of the autocorrelation function of the  $[Ca^{2+}]_i$  spike train. We define the cross-correlation between the stimulus,  $s(t)$ , and the spike train,  $x(t)$ , as

$$R_{sx}(\tau) = \frac{1}{T} \int_0^T dt s(t) x(t + \tau) \quad (10)$$

and the autocorrelation function of the  $[Ca^{2+}]_i$  spike train,  $x(t)$ , as

$$R_{xx}(\tau) = \frac{1}{T} \int_0^T dt x(t) x(t + \tau). \quad (11)$$

The filter,  $h(t)$ , computed from eq. 9 is not causal in general in the sense that  $h(t) \neq 0$  for  $t > 0$ , *i.e.*, the occurrence of a spike can be used to predict the future temporal dynamics of the stimulus (this is of course only possible because of correlations in the stimulus and because of the response properties of the simulated cell). Causality is usually implemented by introducing a time delay into the reconstructions<sup>14</sup> or by applying a causal Wiener–Kolmogorov filter<sup>28</sup>. If no correlations exist between the stimulus,  $s(t)$ , and the spike train,  $x(t)$ , (*i.e.*,  $S_{sx}(f) = 0$  for all frequencies  $f$ ) the best linear estimate of the stimulus,  $s(t)$ , is equal to the mean value,  $\langle s(t) \rangle = 0$ . The maximal mean square error computed from eq. 8 is then equal to the variance of the stimulus,  $\epsilon^2 = \sigma_s^2$ . Once the best linear estimate,  $s_{est}(t)$ , is found, the "noise" contaminating the reconstructions is defined as the difference between the estimated stimulus,  $s_{est}(t)$ , and the stimulus,  $s(t)$ ,

$$n(t) = s_{est}(t) - s(t). \quad (12)$$

The mean square error in the reconstructions<sup>16</sup> is then given by

$$\epsilon^2 = \int_{-f_c}^{f_c} df \frac{S_{ss}(f)}{SNR(f)}, \quad (13)$$

where the signal–to–noise–ratio is defined as

$$SNR(f) = \frac{S_{ss}(f)}{S_{nn}(f)} \geq 1. \quad (14)$$

In this equation  $S_{nn}(f)$  and  $S_{ss}(f)$  are the power spectra of the noise and the stimulus, respectively. Thus the signal–to–noise–ratio,  $SNR(f)$ , is a measure of the amount of signal power present at a given frequency relative to the noise contaminating the reconstructions. In the extreme case where the spike train is completely unrelated to the signal,  $SNR(f) = 1$  for all frequencies, otherwise  $SNR(f) > 1$ .

The accuracy of the reconstruction and thus the information transmitted from the stimulus,  $s(t)$ , to the spike train,  $x(t)$ , is determined by the *coding fraction* defined as

$$\gamma = 1 - \frac{\epsilon}{\sigma}, \quad (15)$$

where  $\epsilon$  is the root–mean–square–error (rmse) between the actual stimulus,  $s(t)$ , and the estimated stimulus,  $s_{est}(t)$ , and  $\sigma$  is the standard deviation of the stimulus,  $s(t)$ <sup>20</sup>. Thus the *coding fraction* represents the percentage of temporal stimulus fluctuations encoded, in units of the stimulus standard deviation. The *coding fraction* takes a maximum value of 1 when the stimulus

is perfectly estimated ( $\epsilon = 0$ ) and the minimum value of 0 if the stimulus estimation from the  $[Ca^{2+}]_i$  spike train is at chance level ( $\epsilon = \sigma$ )<sup>16,30</sup>. The accuracy of encoding in different simulations can be compared on the basis of the *coding fraction*. Bialek and collaborators<sup>14,29</sup> used a different measure, the mutual information transmitted by the reconstructions,  $s_{est}(t)$ , about the stimulus,  $s(t)$ . In contrast to the coding fraction which can be computed for stimuli of arbitrary statistics, the estimation of information rates requires the stimulus to be Gaussian. For a Gaussian white noise stimulus, the  $\epsilon$  – *entropy* or rate of distortion function is defined as

$$I_\epsilon = \frac{-f_c}{\log(2)} \log\left(\frac{\epsilon}{\sigma}\right) \quad (\text{in bit/sec}), \quad (16)$$

and is a measure of the equivalent rate of information transmission<sup>30,31,32</sup>. An absolute lower bound for the rate of information transmitted per  $[Ca^{2+}]_i$  spike is obtained by dividing  $I_\epsilon$  by the mean  $[Ca^{2+}]_i$  spike frequency,  $\lambda$ ,

$$I_s = \frac{I_\epsilon}{\lambda} \quad (\text{in bit/spike}). \quad (17)$$

### 3 Results

In the first step of our analysis we estimated the effective temporal bandwidth of stimulus frequencies encoded in the  $[Ca^{2+}]_i$  spike train using bandlimited Gaussian white noise stimuli with high ( $f_c = 100$  mHz) and low ( $f_c = 10$  mHz) cut-off frequencies. The signal-to-noise ratio (SNR) in the reconstructions was calculated according to eq. 14. Signal-to-noise ratios were equal to 1 for frequencies larger than 20 mHz, *i.e.*, these frequencies were not encoded in the  $[Ca^{2+}]_i$  spike train (Fig. 1A). Short segments of the stimuli, the corresponding reconstructed stimuli, and the  $[Ca^{2+}]_i$  spike train are plotted in (Fig. 1B, C). Using a Gaussian white noise stimulus with a high cut-off frequency,  $f_c = 100$  mHz resulted in a poor estimate of the reconstructed stimulus with a *coding fraction* below 10% ( $\gamma = 0.077$ , Fig. 1B). Choosing a lower cut-off frequency for the Gaussian stimulus ( $f_c = 10$  mHz) which was adjusted to the frequency band encoded by the simulated signal transduction process resulted in a better reconstruction of the stimulus.

This was indicated by higher SNRs for low frequencies (Fig. 1A) and more than 70% of the stimulus were reconstructed ( $\gamma = 0.73$ , Fig. 1C). The reconstruction filters,  $h(t)$ , for both stimuli are displayed in Fig. 1D). In the following step, we systematically investigated the effect of the cut-off frequency,  $f_c$ , on the coding performance by calculating the *coding fraction*,  $\gamma$ , and the *information* transmitted per spike,  $I_s$ , by varying  $f_c$  between 3 mHz and 100 mHz.

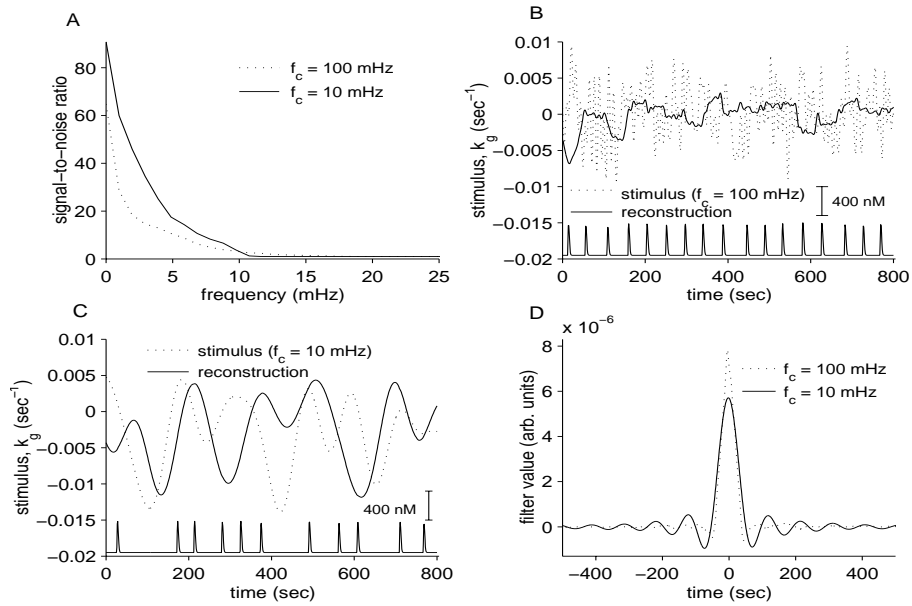


Figure 1: A: Signal-to-noise ratio (SNR) of the reconstructions from  $Ca^{2+}$  spike trains in response to Gaussian white noise stimuli. B: Reconstruction for stimulus with  $f_c = 100$  mHz and C: with  $f_c = 10$  mHz (mean value of  $k_g$  subtracted). Lower traces:  $[Ca^{2+}]_i$  spike trains. D: Reconstruction filters.

The *coding fraction* monotonically decreased with increasing  $f_c$ , whereas the *information* transmitted per spike ( $I_s$ ) kept constant for cut-off frequencies larger than approx. 30 mHz (Fig. 2).

To study the effect of the mean  $[Ca^{2+}]_i$  spike frequency on the coding behavior in our model system, we choose a cut-off frequency of 10 mHz which has been demonstrated to give good reconstructions of the stimulus. The mean amplitude of the Gaussian stimuli ( $f_c = 10$  mHz) was monotonically increased to modulate the mean  $Ca^{2+}$  spike frequency. We found that the *coding fraction* and the *information* transmitted per spike had a maximum of  $\gamma = 0.87$  and  $I_s = 1.1 \text{ bit/spike}$  respectively at a physiologically plausible value of the  $[Ca^{2+}]_i$  spike frequency of 27 mHz (Fig. 3).

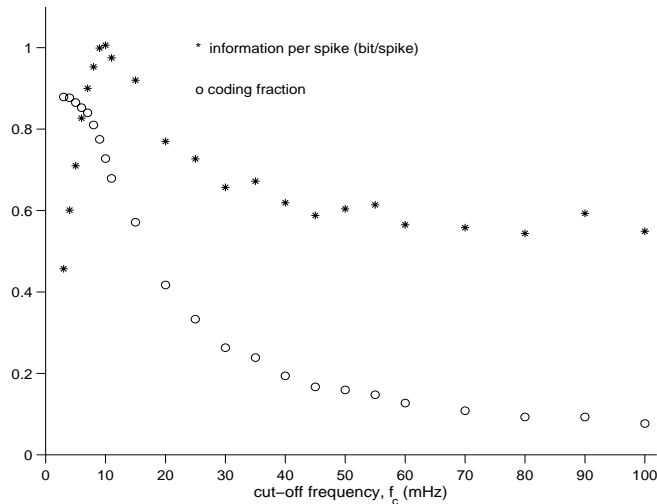


Figure 2: Effect of  $f_c$  on the coding behavior quantified by the *coding fraction* and the *information* transmitted per spike.

#### 4 Discussion

Endocrine systems are regulated dynamically and organized in temporal and structural hierarchies ranging from the pulsatile release of hormones and the fluctuations of hormone concentrations in the blood stream to the oscillations of intracellular concentrations of signaling molecules, such as  $Ca^{2+}$ . The issue of *temporal vs. mean rate coding* which has received a lot of attention in the field of neuroscience in the last couple of years (see ref. 19 for an overview) has not yet been studied in the endocrine system. Information transmission in sensory neuronal systems has been quantified using information-theoretic approaches to stimulus reconstruction from spike trains<sup>14,15,16,19,20</sup>. In the endocrine system experimental and numerical studies have been performed to study the effect of different pulse frequencies (*mean rate coding*) and amplitudes on the regulation of intracellular signaling<sup>10,11</sup> as well as cellular function and structure<sup>33,34</sup>. However, to date experimental as well as numerical studies exploring the effect of timing of hormonal pulses (*temporal coding*) on the regulation of intracellular signaling and target cell function and structure are lacking.

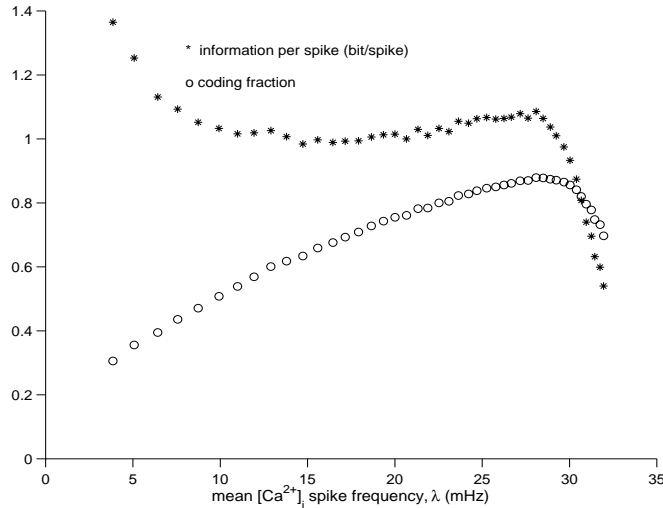


Figure 3: Effect of the mean  $[Ca^{2+}]_i$  spike frequency on the coding behavior quantified by the *coding fraction* and the rate of *information* transmission.

This work represents the first attempt to quantify the information flow in endocrine signaling from the secretory signaling cell to the final effector system of a target cell, exemplified for the subsystem of transmembrane signaling. We used a model of receptor–controlled intracellular  $Ca^{2+}$  oscillations<sup>11</sup> investigated under stimulation by a time–varying random hormonal agonist (bandlimited Gaussian white noise). A stimulus reconstruction method first proposed by Bialek *et al.*<sup>14</sup> and subsequently refined by Gabbiani and Koch<sup>16,30</sup> was applied to estimate the time–varying hormonal input signal from the corresponding  $[Ca^{2+}]_i$  spike train. Two different measures were used to quantify the coding performance of transmembrane signaling in our model system: the *coding fraction*,  $\gamma$  and the rate of information transmitted per  $[Ca^{2+}]_i$  spike,  $I_s$ . The *coding fraction*,  $\gamma$  is used to compare directly the quality of the reconstruction of the stimulus in the time domain. The information transmitted per spike on the other hand reports the effective information transmission in a given frequency band (depending on the cut–off frequency,  $f_c$ ), but it does not directly compare the actual and the reconstructed stimulus. Thus, it is possible to find a value for  $I_s$  of 0.55 bit/sec at  $f_c = 100$  mHz (Fig. 2), although the quality of the reconstruction is poor, since less than 10% ( $\gamma = 0.077$ ; Fig. 2) of the stimulus is encoded in the  $[Ca^{2+}]_i$  spike train. Lowering the cut–off

frequency to  $f_c = 30$  mHz, the  $[Ca^{2+}]_i$  spike train is able to convey more than 25% about the stimulus ( $\gamma = 0.26$ ) at a similar rate of information transmission,  $I_s$ . Thus the amount of information which the spike train conveys about the stimulus stays stable over a broad range of stimuli with different cut-off frequencies whereas the quality of the stimulus reconstruction depends on the dynamics of the time-varying stimulus. The *coding fraction* displayed a peak shaped curve with a maximum at  $f_c = 10$  mHz whereas we got a sigmoidal curve for the rate of information transmitted from the stimulus to the spike train. It will be necessary to verify experimentally the results found in our simulations by using time-varying hormonal stimuli whose bandwidth is matched to the encoding mechanism of the transmembrane signaling system, *i.e.*, in the range from 5 mHz to 30 mHz for  $f_c$  we found the best reconstructions as well as the highest rate of information transmission. This corresponds to a mean interpulse interval of the hormonal stimulus of approx. 30 sec. to 200 sec. Our study leaves the question open to determine whether the information of the time-varying hormonal stimulus that can be encoded in the  $[Ca^{2+}]_i$  spike train is actually used by the target cell. In this context, it would be particularly interesting to correlate the quantitative measures of the coding performance, such as the signal-to-noise ratio, the *coding fraction*, and the *information* transmitted per spike,  $I_s$ , with a measure of the final effector response. Currently, it appears difficult to design and perform such a study which correlates dynamic stimulatory patterns and the final response of a cell. The method used here to quantify the information flow in the subsystem of transmembrane signaling may be used in other parts of the information transmission system from the signaling cell to the final effector system. The convergence of information through the phenomenon of *cross-talk*<sup>1</sup> may lead to an increase of the *coding fraction*. On the other hand, if the *coding fraction* decreases, the stimulus reconstruction could define the features of the stimulus signal that were extracted between two stages of this signaling pathway.

### Acknowledgments

We thank J. van den Hoff for help with the manuscript. This work was supported by DFG under grants Scho 466/1-3, Br 915/4-2, and Pr 333/8-1.

### References

1. C. Schöfl *et al.*, *Trends Endocrinol. Metab.* **5**, 53 (1994).
2. M. Berridge and A. Galione, *FASEB J.* **2**, 3074 (1988).
3. M.D. Bootman and M.J. Berridge, *Cell* **83**, 675 (1995).

4. A. Ghosh *et al.*, *Science* **263**, 1618 (1994).
5. H. Bading *et al.*, *Science* **260**, 181 (1993).
6. X. Gu, N.C. Spitzer, *Nature* **375**, 784 (1995).
7. H.T. Cline, R.W. Tsien, *Neuron* **6**, 259 (1991).
8. G. Brabant *et al.*, *Trends Endocrinol. Metab.* **3**, 183 (1992).
9. E. van Cauter and F.W. Turek in *Endocrinology*, ed. L. J. DeGroot (W.B. Saunders Company, Philadelphia, 1995).
10. C. Schöfl *et al.*, *Am. J. Physiol.* **265**, C1030 (1993).
11. T.R. Chay *et al.*, *J. theor. Biol.* **174**, 21 (1995).
12. K.S.R. Cuthbertson and T.R. Chay, *Cell Calcium* **12**, 97 (1991).
13. K. Prank *et al.*, *Phys. Rev. Lett.* **77**, 1909 (1996).
14. W. Bialek *et al.*, *Science* **252**, 1854 (1991).
15. F. Gabbiani *et al.*, *Nature* **384**, 564 (1996).
16. F. Gabbiani and C. Koch, *Neural Comput.* **8**, 44 (1996).
17. F. Theunissen *et al.*, *J. Neurophysiol.* **75**, 1345 (1996).
18. F. Rieke, D. Warland, R.R.D. van Steveninck and W. Bialek, *Spikes: Exploring the Neural Code* (MIT Press, Cambridge, MA, 1997).
19. F. Rieke *et al.*, *Proc. R. Soc. London B* **262**, 259 (1995).
20. R. Wessel *et al.*, *J. Neurophysiol.* **75**, 2280 (1996).
21. E.N. Eskandar *et al.*, *J. Neurophysiol.* **68**, 1277 (1992).
22. W. Singer, C.M. Gray, *Ann. Rev. Neurosci.* **18**, 555 (1995).
23. R.C. Decharms, M.M. Merzenich, *Nature* **381**, 610 (1996).
24. G. Laurent, *Trends Neurosci.* **19**, 489 (1996).
25. M. Wehr, G. Laurent, *Nature* **384**, 162 (1996).
26. J.E. Lisman, *Trends Neurosci.* **20**, 38 (1997).
27. N. Wiener, *Extrapolation, Interpolation and Smoothing of Stationary Time Series*. (John Wiley & Sons, New York, 1949).
28. H.V. Poor, *An Introduction to Signal Detection and Estimation*. 2<sup>nd</sup> ed. (Springer-Verlag, New York, 1994).
29. F. Rieke *et al.*, *Europhys. Lett.* **22**, 151 (1993).
30. F. Gabbiani, *Network Comp. Neural Syst.* **7**, 61 (1996).
31. A.N. Kolmogorov, *IRE Trans. Inform. Theory* **2**, 102 (1956).
32. C.E. Shannon in *The mathematical theory of communication*, ed. C.E. Shannon and W. Weaver (Illinois University Press, Urbana, IL, 1963).
33. D.J. Haisenleder, *Endocrinology* **130**, 2917 (1992).
34. M.A. Shupnik, *Mol. Endocrinology* **4**, 1444 (1990).